

# Geometric Quantum Computation with NMR

<sup>\*†</sup>Jonathan A. Jones, <sup>\*</sup>Vlatko Vedral, <sup>\*</sup>Artur Ekert and <sup>‡</sup>Giuseppe Castagnoli

<sup>\*</sup>*Centre for Quantum Computation, Clarendon Laboratory, Parks Road, Oxford OX1 3PU, UK*

<sup>†</sup>*OCMS, New Chemistry Laboratory, South Parks Road, Oxford OX1 3QT, UK*

<sup>‡</sup>*Elsag, Via Puccini 2, 1615 Genova, Italy*

(May 5, 2019)

An exciting recent development has been the discovery that the computational power of quantum computers exceeds that of Turing machines [1]. The experimental realisation of the basic constituents of quantum information processing devices, namely fault-tolerant quantum logic gates, is a central issue. This requires conditional quantum dynamics, in which one subsystem undergoes a coherent evolution that depends on the quantum state of another subsystem [2]. In particular, the subsystem may acquire a conditional phase shift. Here we consider a novel scenario in which this phase is of geometric rather than dynamical origin [3,4]. As the conditional geometric (Berry) phase depends only on the geometry of the path executed it is resilient to certain types of errors, and offers the potential of an intrinsically fault-tolerant way of performing quantum gates. Nuclear Magnetic Resonance (NMR) has already been used to demonstrate both simple quantum information processing [5–9] and Berry’s phase [10–12]. Here we report an NMR experiment which implements a conditional Berry phase, and thus a controlled phase shift gate. This constitutes the first elementary geometric quantum computation.

Any quantum computation can be build out of simple operations involving only one or two quantum bits (qubits) [13]. A particularly simple two qubit gate in many experimental implementations, such as NMR [14], is the controlled phase shift. This may be achieved using a conditional Berry phase, and thus quantum geometrical phases can form the basis of quantum computation. We will use spin half nuclei as an example to demonstrate the

feasibility of this approach, but the basic idea is completely general. In our experiments the state of one spin determines the Berry phase acquired by the other spin.

Suppose that a spin half nucleus undergoes a conical evolution with cone angle  $\theta$ . Then the Berry phase is simply  $\gamma = \pm\frac{1}{2}\Omega = \pm\pi(1 - \cos\theta)$  where the  $\pm$  signs depend on whether the system is in the eigenstate aligned with or against the field, and  $\Omega$  is the solid angle subtended by the conical circuit. Note that any deformation of the path of the spin which preserves this solid angle leaves the phase unchanged. Thus the phase is not affected by the speed with which the path is traversed; nor is it very sensitive to random fluctuations about the path.

Berry phases can be conveniently demonstrated in an NMR experiment [15] by working in a rotating frame. Consider an ensemble of spin half particles in a magnetic field,  $B_0$ , aligned along the  $z$ -axis; their precession frequency is then given by the Larmor frequency,  $\omega_0$ . If the spins are irradiated by a circularly polarized RF field,  $B_1$ , at a frequency  $\omega_{\text{rf}}$  the total Hamiltonian (neglecting relaxation) may be written in the rotating frame as  $\mathcal{H} = (\omega_0 - \omega_{\text{rf}}) I_z + \omega_1 I_x$ , where, following conventional NMR practice, the Hamiltonian is described in product operator notation [16] and the field strengths are written in terms of their corresponding Larmor frequencies.

When  $|\omega_1| \ll |\omega_0 - \omega_{\text{rf}}|$  the Hamiltonian lies close to the  $z$ -axis, while when  $|\omega_1| \gg |\omega_0 - \omega_{\text{rf}}|$ , the Hamiltonian lies close to the  $x$ -axis. If RF radiation is applied far from resonance, the system is effectively quantized along the  $z$ -axis, and if the RF frequency is swept towards resonance ( $\omega_{\text{rf}} = \omega_0$ ), the effective Hamiltonian rotates from the  $z$ -axis towards the  $x$ -axis. If the frequency sweep is applied adiabatically then the spin will follow the Hamiltonian. Next, a circular motion can be imposed by adiabatically varying the phase of the RF. When the Hamiltonian returns to the  $x$ -axis the frequency sweep may be reversed, so that the spin returns to its original state, aligned along the  $z$ -axis. The Berry phase acquired in this cyclic process is  $\pm\pi$ . If the RF field is not swept all the way to resonance, but only to some final value  $\omega_f$ , the Hamiltonian ends at some angle to the  $z$ -axis, and so circuits with arbitrary cone angles can be implemented. A similar case occurs

if the frequency sweep is replaced by an amplitude sweep, in which the RF is always applied away from resonance, and its amplitude is raised smoothly from zero to some final value,  $\omega_1$ .

This situation arises naturally in a system of two weakly coupled spins,  $I$  and  $S$ . For simplicity we consider a heteronuclear system, so that  $\omega_I$  and  $\omega_S$  are very different, and only one spin (say  $I$ ) is close to resonance. The two transitions of  $I$  (corresponding to the two possible states of spin  $S$ ) will be split by  $\pm\pi J$ , and so will have different resonance offsets. After an amplitude sweep the orientation of the effective Hamiltonian depends on the resonance offset, and so  $\theta$  (and hence the Berry phase acquired) will depend on the state of spin  $S$ . This permits a conditional Berry phase to be applied to spin  $I$ , where the size of the phase shift is controlled by spin  $S$ . If the RF is applied at a frequency  $\delta$  (measured in Hz) away from the transition frequency of spin  $I$  when spin  $S$  (the control spin) is in state 0, and  $\nu_1$  is the maximum RF field strength (also in Hz), then the differential Berry phase shift,

$$\Delta\gamma = \gamma_1 - \gamma_0 = \pm\pi \left[ \frac{\delta + J}{\sqrt{(\delta + J)^2 + \nu_1^2}} - \frac{\delta}{\sqrt{\delta^2 + \nu_1^2}} \right],$$

depends only on  $\delta$ ,  $\nu_1$  and  $J$ ; it is independent of how the process is carried out as long as it is slow enough to be adiabatic, but rapid compared with the decoherence times ( $T_1$  and  $T_2$ ).

In addition to the geometric phases, there will also be additional dynamic phases, which *do* depend on experimental details. In principle these could be calculated and corrected for, but this is not practical as a result of  $B_1$  inhomogeneity. The RF field strength will vary over the sample, and so different nuclei will acquire different dynamic phases; averaging over the sample will result in extensive dephasing. This can be overcome using a conventional spin echo approach: the pulse sequence is applied twice, with the second application surrounded by a pair of  $180^\circ$  pulses applied to spin  $I$ . This has the effect of completely refocussing the dynamic phase, and thus refocussing any inhomogeneity in it. This procedure would also cancel out the geometric phase, but this can be side stepped by performing the RF phase

sweep in the *opposite* direction, thus negating the geometric phase, so that the two geometric terms add together while the dynamic phases cancel out. Cancellation of dynamic phases arising from the natural evolution of spin  $S$ , could also be achieved by incorporating the sequence within another spin echo, involving  $180^\circ$  pulses applied to  $S$ . Similarly, in more complex spin systems, contributions to the geometric phase which depend on the states of other spins can be cancelled by the judicious application of further spin echoes.

In order to measure the sizes of  $\gamma_0$  and  $\gamma_1$  it is convenient to apply the Berry phase shifts to a spin  $I$  in a coherent superposition of states, created by an initial  $90^\circ$  pulse. The pulse sequence (figure 1) then generates Berry phases that are determined by examining the final phase of the magnetisation. As the 2 states of spin  $I$  acquire equal and opposite phases, and the pulse sequence contains two separate periods in which phase shifts are generated, the total phase change observed is  $4\gamma$ , with a maximum value of  $720^\circ$ . A range of controlled Berry phases can be generated by choosing appropriate values of  $\delta$  and  $\nu_1$  ( $J$  is fixed by the chemical system). For a given value of  $\delta/J$  the controlled phase will rise and then fall as  $\nu_1$  is increased. Clearly this approach will be most robust when the desired  $\Delta\gamma$  occurs at the maximum of this curve, as the dependence on the size of  $\delta$  is then reduced to second order. For the particular case of a controlled  $\pi$  shift, the basis of the controlled-NOT gate [14], this occurs at  $\delta = 1.058J$  and  $\nu_1 = 2.112J$ .

NMR experiments were performed at  $25^\circ\text{C}$  using a homebuilt 500 MHz ( $^1\text{H}$ -frequency) NMR spectrometer at the OCMS, with two power ranges for  $^1\text{H}$  pulses. Hard pulses were applied using high power ( $\nu_1 < 25.8\text{ kHz}$ ), while adiabatic sweeps were performed using low power ( $\nu_1 < 774\text{ Hz}$ ). RF amplitude and phase calibration tables (available on most modern NMR spectrometers) permit the RF power level to be varied in a phase coherent manner. The sample was prepared by dissolving 100 mg of 99%  $^{13}\text{C}$  labelled  $\text{CHCl}_3$  in 0.2 ml of 99.96%  $\text{CDCl}_3$ , and placing this in a Shigemi microtube. The single  $^1\text{H}$  nucleus was used as spin  $I$ , while the  $^{13}\text{C}$  nucleus was used as spin  $S$ ; for this system  $J_{IS} = 209.2\text{ Hz}$ . Experiments were performed with  $\delta = 221.3\text{ Hz}$ , and  $\nu_1$  was varied between zero and its maximum value. Amplitude and phase sweeps were implemented using 200 linear steps of

$100\,\mu\text{s}$ , giving a total pulse sequence length of about  $120\,\text{ms}$ . The phases of the two  $^1\text{H}$  resonances were determined by fitting the free induction decay using home-written software. Reference phases were obtained as described in the caption of figure 1. The results are shown in figure 2; clearly the measured phases lie close to the theoretically predicted values. The controlled Berry phase rises smoothly to a broad maximum at  $180^\circ$ , and then slowly falls back towards zero. In order to investigate the effects of a breakdown in the adiabatic criterion, some measurements were repeated with faster sweeps. With a sweep step size of  $50\,\mu\text{s}$  (data not shown) the results were similar to, but not quite as good as, those obtained with the slower sweep. Below  $50\,\mu\text{s}$  the loss of adiabaticity is severe and major distortions are observed. The step size should not be increased too far beyond the adiabatic threshold, as this will increase the effects of decoherence.

The conditional Berry phase gate demonstrated here depends only on the geometry of the path, and is completely independent of how the motion is performed as long as it is adiabatic; hence this kind of computation may be called geometric quantum computation. While this approach has no particular advantage over more conventional methods in NMR quantum computation, the basic idea is completely general, and could be applied in other implementations. Some of the methods described here have been partly foreshadowed in previous theory papers (*e.g.*, [17,18]), but this is the first clear theoretical description and experimental demonstration of such effects. This new approach to quantum gates may be important in the future, as it is naturally resilient to *certain* types of errors. In particular, suppose that the qubit, in addition to the circular motion which implements the geometric phase, also undergoes a random motion about its path due to some unwanted interaction with the environment. Such noisy motion leaves the total area approximately unchanged (although it changes details of the path), and so will not be reflected in the final Berry phase. Geometric phases thus offer the potential of performing quantum computations in a manner which is naturally tolerant of some types of fault. Further generalizations to non-abelian Berry phases, if implemented, may open entirely new possibilities for robust quantum information processing [19,20].

## REFERENCES

- [1] Shor, P. W. Polynomial-Time Algorithms for Prime Factorization and Discrete Logarithms on a Quantum Computer. *SIAM Review* **41**, 303–332 (1999).
- [2] Barenco, A., Deutsch, D., Ekert, A. & Jozsa, R. Conditional Quantum Dynamics and Logic Gates. *Phys. Rev. Lett.* **74**, 4083–4086 (1995).
- [3] Berry, M. V. Quantal phase factors accompanying adiabatic changes. *Proc. Roy. Soc. A* **392**, 45–57 (1984).
- [4] Shapere, A. & Wilczek, F. *Geometric Phases in Physics* (World Scientific, Singapore, 1989)
- [5] Cory, D. G., Fahmy, A. F. & Havel, T. F. Ensemble quantum computing by NMR spectroscopy *Proc. Nat. Acad. Sci. USA* **94**, 1634–1639 (1997).
- [6] Gershenfeld, N. A. & Chuang, I. L. Bulk spin-resonance quantum computation. *Science* **275**, 350–356 (1997).
- [7] Jones, J. A. & Mosca, M. Implementation of a quantum algorithm on a nuclear magnetic resonance quantum computer. *J. Chem. Phys.* **109**, 1648–1653 (1998).
- [8] Chuang, I. L., Gershenfeld, N. & Kubinec, M. Experimental implementation of fast quantum searching. *Phys. Rev. Lett.* **80**, 3408–3411 (1998).
- [9] Cory, D. G., Price, M. D. & Havel, T. F. Nuclear magnetic resonance spectroscopy: An experimentally accessible paradigm for quantum computing. *Physica D* **120**, 82–101 (1998).
- [10] Suter, D., Chingas, G., Harris, R. & Pines, A. Berry’s phase in magnetic resonance. *Mol. Phys.* **61**, 1327–1340 (1987).
- [11] Goldman, M., Fleury, V. & and Guéron, M. NMR frequency shift under sample spinning. *J. Magn. Reson. A* **118**, 11–20 (1996).

[12] Jones, J. A. & Pines, A. Geometric Dephasing in Zero-Field Magnetic Resonance. *J. Chem. Phys.* **106**, 3007–3016 (1997).

[13] Deutsch, D., Barenco, A. & Ekert, A. Universality in Quantum Computation. *Proc. Roy. Soc. A* **449**, 669–677 (1995).

[14] Jones, J. A., Hansen, R. H. & and Mosca, M. Quantum Logic Gates and Nuclear Magnetic Resonance Pulse Sequences. *J. Magn. Reson.* **135**, 353–360 (1998).

[15] Ernst, R. R., Bodenhausen, G. & Wokaun, A. *Principles of Nuclear Magnetic Resonance in One and Two Dimensions* (Clarendon Press, Oxford, 1987).

[16] Sørensen, O. W., Eich, G. W., Levitt, M. H., Bodenhausen, G. & Ernst, R. R. Product Operator-Formalism for the Description of NMR Pulse Experiments. *Prog. NMR Spectrosc.* **16**, 163–192 (1983).

[17] Pellizzari, T., Gardiner, S. A., Cirac, J. I. & Zoller, P. Decoherence, Continuous Observation, and Quantum Computing: A Cavity QED Model. *Phys. Rev. Lett.* **75**, 3788–3791 (1995).

[18] Averin, D. V., Adiabatic Quantum Computation with Cooper Pairs. *Solid State Commun.* **105**, 659–664 (1998).

[19] Kitaev, A. Y. Fault tolerant quantum computation with anyons. LANL e-print quant-ph/9707021.

[20] Preskill, J. Fault tolerant quantum computation. LANL e-print quant-ph/9712048.

#### ACKNOWLEDGEMENTS

Theory was developed by V.V, A.E., and G.C.; NMR experiments were developed and performed by J.A.J. We thank N. Soffe for helpful discussions. J.A.J. and A.E. are Royal Society Research Fellows. J.A.J. and A.E. thank Starlab (Riverland NV) for financial support. Correspondence should be addressed to J.A.J. (e-mail: [jonathan.jones@qubit.org](mailto:jonathan.jones@qubit.org)).

## FIGURES

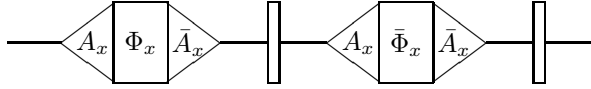


FIG. 1. Pulse sequence used to demonstrate controlled Berry phases. Triangles indicate adiabatic RF amplitude sweeps, from 0 to  $\nu_1$  ( $A_x$ ) or *vice versa* ( $\bar{A}_x$ ), while rectangles indicate slow rotations of the RF phase at constant amplitude; the phase rotation runs from 0 to  $360^\circ$  ( $\Phi_x$ ) or from  $360$  to  $0^\circ$  ( $\bar{\Phi}_x$ ). Narrow rectangles correspond to hard  $180^\circ_y$  pulses. As the absolute phase of an NMR signal is undefined, it is essential to obtain a reference signal against which experimental phases can be measured. The simplest approach is to use the signal from a single  $90^\circ$  pulse, while a more subtle approach is to use this pulse sequence with the  $\bar{\Phi}_x$  sequence replaced by  $\Phi_x$ . In principle these should give the same result, but in practice minor differences are seen as a result of RF inhomogeneity and the effects of the long RF pulses on the NMR probe and pre-amplifier.

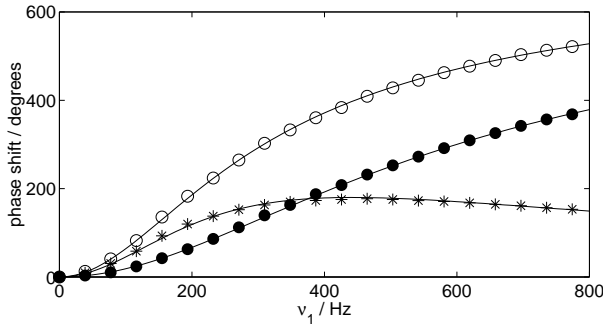


FIG. 2. Experimental results:  $\gamma_0$ ,  $\gamma_1$ , and the controlled Berry phase,  $\Delta\gamma$ , as a function of  $\nu_1$ . Experimental points are shown by circles, the phase difference is shown by stars, and theoretical values are shown as smooth curves. Variability in the experimental points (estimated by repetition) was about  $\pm 2^\circ$ ; in a few cases the deviation of the measured data points from their theoretical values was greater than this, indicating the existence of as yet unidentified systematic errors.